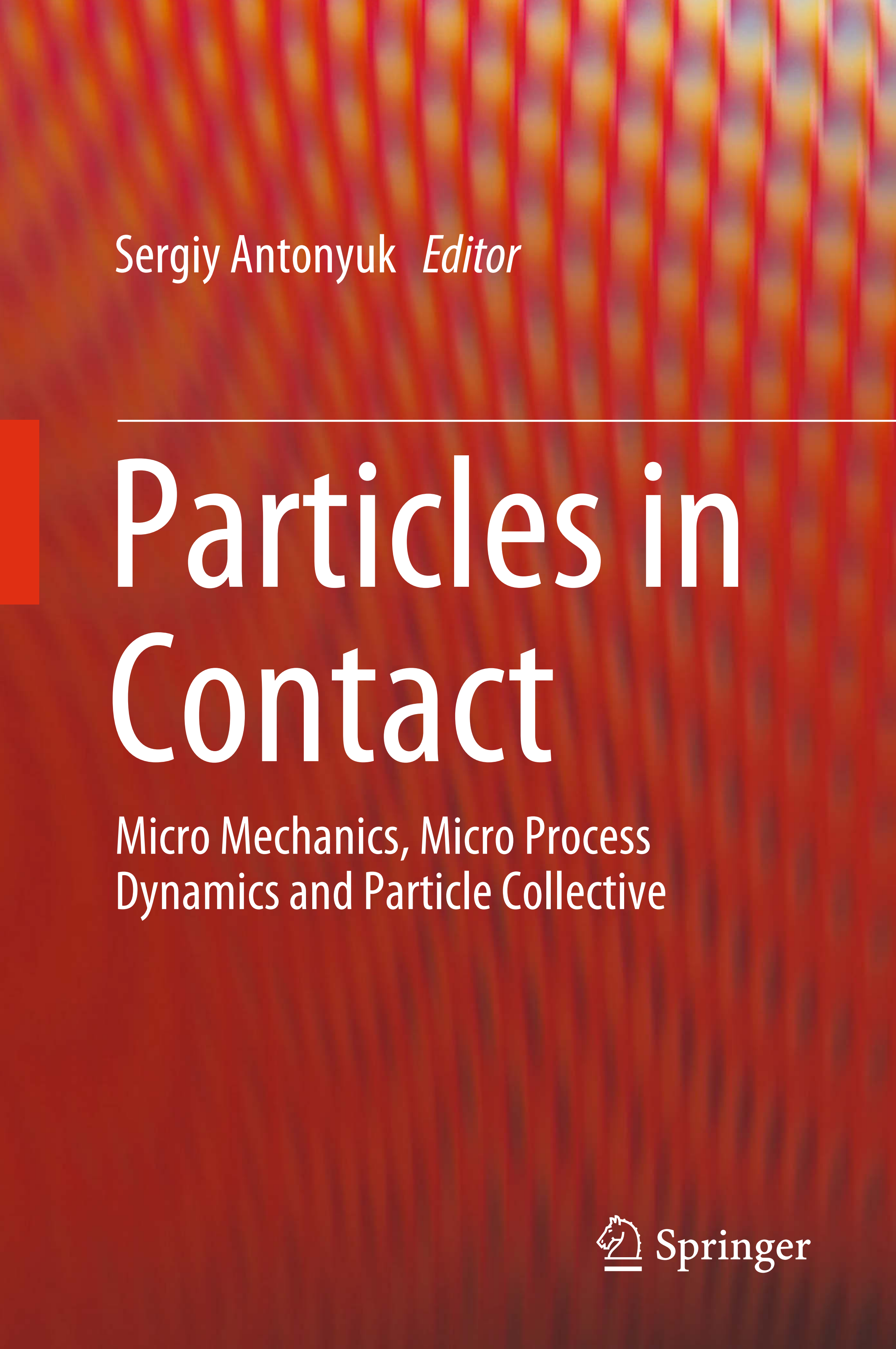

Sergiy Antonyuk *Editor*

Particles in Contact

Micro Mechanics, Micro Process Dynamics and Particle Collective

Springer

Particles in Contact

Sergiy Antonyuk
Editor

Particles in Contact

Micro Mechanics, Micro Process Dynamics and Particle Collective

Springer

Editor
Sergiy Antonyuk
Institute of Particle Process Engineering
Technische Universität Kaiserslautern
Kaiserslautern, Germany

ISBN 978-3-030-15898-9 ISBN 978-3-030-15899-6 (eBook)
https://doi.org/10.1007/978-3-030-15899-6

© Springer Nature Switzerland AG 2019
This work is subject to copyright. All rights are reserved by the Publisher, whether the whole or part of the material is concerned, specifically the rights of translation, reprinting, reuse of illustrations, recitation, broadcasting, reproduction on microfilms or in any other physical way, and transmission or information storage and retrieval, electronic adaptation, computer software, or by similar or dissimilar methodology now known or hereafter developed.
The use of general descriptive names, registered names, trademarks, service marks, etc. in this publication does not imply, even in the absence of a specific statement, that such names are exempt from the relevant protective laws and regulations and therefore free for general use.
The publisher, the authors and the editors are safe to assume that the advice and information in this book are believed to be true and accurate at the date of publication. Neither the publisher nor the authors or the editors give a warranty, expressed or implied, with respect to the material contained herein or for any errors or omissions that may have been made. The publisher remains neutral with regard to jurisdictional claims in published maps and institutional affiliations.

This Springer imprint is published by the registered company Springer Nature Switzerland AG
The registered company address is: Gewerbestrasse 11, 6330 Cham, Switzerland

This book is dedicated in memory of
Professor Jürgen Tomas—an outstanding
scientist, colleague and friend.

Preface

The properties and behaviour of particulate products, such as powder materials, agglomerated or coated materials, fillers, active ingredients or pigments and natural substances, like soils, sludge or aerosols, are significantly determined by interactions between fine solid particles in granular matter. The production, handling and transport processes of the solid products are also heavily influenced by the interparticle interactions. For the optimization of existing solid processes and development of novel particulate products, the understanding and description of physicochemical microprocesses, which take place during approaching, direct contact and detachment of adhesive fine particles (from a few nanometers to 100 micrometers) are needed. Therefore, the description of macroscopic phenomena and properties of particulate matter consisting of many particles needs a basic understanding of the micromechanical and adhesive interactions of single particles in contact. They can be characterized by stress–strain, force–displacement, torgue–angle and potential–distance relationships for six degrees of freedom for the translation and rotation of particles in contact. New scientific developments in the field of simulations as well as measuring technique make it possible to understand and describe these relationships in the form of contact or potential models. These interaction models based on the physical parameters of individual particles can be used in modern particle-based simulation methods, such as Discrete Element Method or Molecular Dynamics, to provide an accurate prediction of the morphology, microstructure, deformation and flow behaviour and distribution of the properties of particulate systems in industrial processes.

The German Research Foundation (Deutsche Forschungsgemeinschaft, DFG) has supported an international research program in the form of Priority Program (SPP 1486) “Particles in Contact—Micro Mechanics, Micro Process Dynamics and Particle Collective” from 2010 to 2017. This book summarizes the research results of this joint research project obtained by 27 cooperating institutes from Germany, Austria, The Netherlands and Switzerland. The coordinator of this program was Prof. Jürgen Tomas from the Otto von Guericke University Magdeburg (Germany). This program was created and successfully carried out thanks to his innovative ideas, his enthusiasm for powder technology that has brought the scientists from different research areas together into this research project. Unfortunately, he passed away too early. Since 2015, Prof. Sergiy Antonyuk from the Technische Universität Kaiserslautern has taken over the coordination of this program.

We want to thank DFG for the financial support, and specially Dr.-Ing. Bernd Giernoth, Dr.-Ing. Georg Bechtold, Dr. Simon Jörres and Ms. Anja Kleefuß for their excellent coordination and support for the research activities of the SPP.

I am grateful to my Ph.D. students Vanessa Puderbach, Robert Hesse, Philipp Lösch, Dominik Weis, and Oleg Urazmetov, who caught misprints in the proofs of this book.

Kaiserslautern, Germany Sergiy Antonyuk
December 2018

Contents

Analysis of Adsorbates and Interfacial Forces at Metal Oxide Interfaces at Defined Environmental Conditions

A. G. Orive, C. Kunze, B. Torun, T. de los Arcos and G. Grundmeier

Introduction

Adhesion forces between ensembles of micro- and nanoparticles are central in processes such as fluidization, agglomeration and sintering [1]. These effects find applications in an extensive range of technical fields that include the development of pharmaceutical powders, paints, and solar cells [2, 3].

Contact forces between oxide nanoparticles are strongly dependent on the surface chemistry, the presence of adsorbate layers and the environmental conditions [4]. High-energy oxide surfaces under ambient conditions spontaneously adsorb organic molecules and water. This adsorption leads to reduced surface energies. While the existence of atmospheric contaminations on oxide surfaces is routinely observed in surface analytical studies, their surface concentration and composition is often not perfectly controlled.

For most technological applications, assemblies of micro and nanoparticles will be necessarily utilized under normal ambient experimental conditions. As a consequence, the prevalence of water layers adsorbed onto the particle surfaces which are in contact with humid air needs to be taken into account. Indeed, capillary forces due to capillary condensation are particularly interesting since, when present, they usually dominate the inter-particle adhesion interactions. Over the last few years, both theoretical and experimental approaches have been carried out to propose a unified model which might account for the relevance of contact forces between particles under humid conditions [5, 6]. In particular the high-energy surfaces of micro- and nano-metal oxide particles experience the spontaneous adsorption of molecule

---

A. G. Orive · C. Kunze · B. Torun · T. de los Arcos · G. Grundmeier (✉)
Institute of Technical and Macromolecular Chemistry, University Paderborn, Paderborn, Germany
e-mail: g.grundmeier@tc.upb.de; guido.grundmeier@uni-paderborn.de

S. Antonyuk (ed.), *Particles in Contact*,
https://doi.org/10.1007/978-3-030-15899-6_1

adsorbates and water, which gives rise to a reduced surface energy. At this point, it is worth noting that although the afore-mentioned molecular adsorptions due to atmospheric exposure are well-known and easily identified by analytical techniques in interfacial surface studies, their quantitative surface concentration and composition is often not stated or it is poorly characterized. In particular, nano-contact force studies carried out at gas/solid interfaces, e.g. by means of atomic force microscopy (AFM), are often performed upon rather ill-defined conditions.

The quantification of the contact forces occurring between micro- and nanoparticles can be straightforwardly assessed by force spectroscopy measurements by means of AFM [7]. In a seminal contribution, Harrison et al. [8] collected experimental and theoretical results coming from 28 different approaches dealing with the assessment of capillary forces in the nanoparticle regime. It was clearly stated that the impact of capillary forces on particle interfacial adhesion depends on a nontrivial combination of the particle shape, size, deformability, adsorbate layers, surface roughness and hydrophilicity [6, 9]. Indeed, Farshchi-Tabrizi et al. [7] showed that the contact geometry has a critical influence on the humidity dependence of the adhesion force. They addressed the contact forces occurring between regular AFM tips and also the result of attaching particles to them and different solid samples, smooth and rough surfaces. Interestingly, the dependence between adhesion forces and humidity register for hydrophilic surfaces exhibited two distinct behaviors: a maximum or an increasing linear growing behavior. A new numerical models considering both surface roughness and cantilever shape that accurately estimates the quantification of the meniscus force was successfully proposed.

Regarding the presence of molecule adsorbate layers, Gojzewski et al. [10] elegantly introduced the measurement of the contact forces arising between the surfaces of silicon nitride AFM cantilevers and self-assembled monolayers (SAM) on gold as a function of relative humidity by means of dynamic force spectroscopy. Methylene- and hydroxyl-terminated SAMs were used as model hydrophobic and hydrophilic surfaces, respectively. The adhesion forces registered for the hydrophilic SAMs were noticeably higher than those obtained for the hydrophobic ones, even at low humidity values. The latter cannot be thus not only attributed to the formation of hydrogen bridges between hydroxyl groups from the SAM and silanol functionalities of the AFM tip, but also to the strength of the capillary forces.

Taking all the afore-mentioned facts into account, it is clear that AFM measurements carried out under ultra-high vacuum or clean (pure) electrolytes offer the advantage of working with a precisely defined interface chemistry. The aim of the work presented here was to analyze (characterize) the impact of poorly defined ambient surface contamination such as water and organic molecule adsorbates by directly removing them or replacing them by model adsorbates. In the following, TiO_2, ZnO and Al_2O_3 surfaces have been considered as model metal oxides with high surface energy as promising candidates/platforms for fundamental adhesion force studies. In particular, AFM-based methods such as nanoshaving (AFM scratching), UHV-based nanocontact force studies and single molecule force spectroscopy were applied. In addition, in situ FTIR surface spectroscopy was performed to analyze the behavior of some molecule adsorbates under humid conditions.

Materials and Methods

Materials and Surface Preparation

Materials and Chemicals

Rutile TiO_2 single crystals with crystallographic (100) and (110) orientations in the size of 10 mm × 10 mm × 0.5 mm were obtained from *Mateck GmbH* (Juelich, Germany) and *CrysTec* (Germany), respectively. Al_2O_3(11–20) single crystalline substrates of 20 mm × 20 mm × 0.5 mm were also purchased from *Mateck GmbH* (Juelich, Germany).

All chemicals were of p.a. grade (analytical reagent grade) and used without any further purification. Nonadecanoic acid (97%) was purchased from *Fluka.* Octadecylphosphonic acid (97%) and hexylphosphonic acid were obtained from *Alfa Aesar*. α-Mercapto-ω-amino PEG hydrochloride ($HS–PEG–NH_2 \times HCl$, PEG-MW: 10,000 Da), α-Hydroxy-ω-mercapto PEG ($HO–PEG–NHCO–CH_2–CH_2–SH$, PEG-MW: 10,000 Da), α-Methoxy-ω-mercapto PEG ($CH_3O–PEG–SH$, PEG-MW: 10,000 Da) were acquired form *Rapp Polymere GmbH.* Absolute ethanol, used as a solvent and for general cleaning purposes, was purchased from *VWR International*. Hydrofluoric acid (40%) was obtained from Merck *KGa*. Ultrapure water was obtained from an *Ultraclear TWF* (SG Wasseraufbereitung, Barsbüttel, Germany) system with a maximum electrical conductance of 0.055 $\mu S\ cm^{-1}$. RCA-1 solution, i.e. 5:1:1; purified water, ammonia solution 30%, hydrogen peroxide 30%, was used for both etching and cleaning purposes.

Preparation of Rutile TiO_2(110) and (110) Single Crystalline Surfaces [11, 12]

In order to prepare surfaces stable under ambient conditions, TiO_2(100) single crystalline surfaces were prepared from commercial TiO_2 rutile single crystals. The procedure followed consisted of a pre-cleaning step, where the TiO_2 crystals were sonicated in ultrapure water, followed by wet chemical etching, and finally an annealing step according to the methodology developed by Nakamura et al. [13] and Yamamoto et al. [14]. In order to avoid possible contamination of the crystals during the preparation, the etching was performed in a PTFE vessel. (100) and (110) oriented TiO_2 crystals were etched in 20% HF solution for 20 min. After the etching process, the crystals were intensively rinsed with ultrapure water and dried in a stream of pure nitrogen gas. The crystals were then deposited into a tube furnace with Al_2O_3 walls and annealed at 680 °C for 48–72 h in ambient air. A slow heating and cooling rate of 3 °C/min (ramping time of 3.5 h) was selected in order to minimize both mechanical stress in the crystal and in the furnace tube. The quality of the so-prepared TiO_2(100) and (110) single crystals was finally assessed by means of AFM and LEED. A nonconventional 1 × 3 superstructure was obtained in the LEED pattern registered for the as-prepared $TiO_2(100)$ surfaces.

Preparation of $Al_2O_3(0001)$ and (11–20) Single Crystals [11]

In order to produce well-defined $Al_2O_3(0001)$ and $Al_2O_3(11–20)$ single crystalline surfaces, alkaline and acidic etching procedures were applied to the as-received commercial substrates according to a well-established methodology published elsewhere [11]. Briefly, the as-received substrates were immersed into RCA-1 (5:1:1; purified water, ammonia solution 30%, hydrogen peroxide 30%) solution for 2 min at 70 °C to remove organic contaminants. Then, they were subsequently immersed into a phosphoric acid (85%) aqueous solution for 2 min, rinsed with ultra-pure water, and dried with nitrogen. The as-treated crystals were then annealed under an ambient atmosphere at 1450 °C for 36 h.

Additionally, in the case of $Al_2O_3(11–20)$ the single crystals were again immersed into phosphoric acid (85%, 2 min), rinsed with ultra-pure water, and dried with nitrogen. The goal was to simulate the acidic treatment conventionally used in the conditioning Al-alloy surfaces before being exposed to adhesive compounds. A representative AFM image of such prepared surfaces is shown in Fig. 1.

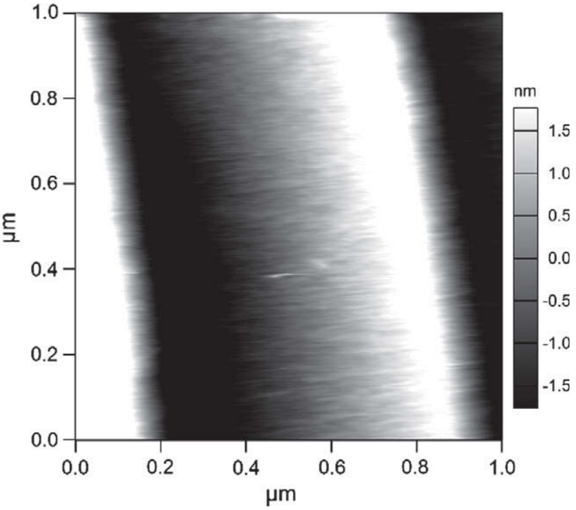

Fig. 1 AFM topography image of $Al_2O_3(11–20)$ single crystal cleaned with RCA-1, etched with concentrated phosphoric acid, heat treated at 1450 °C, and finally etched in concentrated phosphoric acid. Reprinted from [15] with permission from Elsevier

Adsorption of Organic Monolayers on TiO_2 and Al_2O_3 Single Crystalline Surfaces [11]

In order to carry out fundamental studies about the interaction between carboxylic acids with well-defined TiO_2 surfaces, nonadecanoic acid (NDCA) was selected as a model system to characterize the adsorbate formation process onto TiO_2(100) single crystalline substrates [11]. In this regard, freshly prepared TiO_2 single crystals were immersed into a 1 mM NDCA ethanolic solution for 12–16 h. After that, the as-modified substrates were rinsed in ethanol and dried in a nitrogen stream.

Additionally, with the aim to remove the scarcely defined carbon contaminations due to atmospheric contamination, TiO_2(110) substrates were chemically modified by self-assembly (SA) with octadecylphosphonic acid (ODPA) molecule layer. In this regard, freshly prepared and annealed TiO_2(110) single crystals were immersed into a 1 mM ODPA ethanolic solution for 16 h. The as-modified substrates were thoroughly rinsed in ethanol and dried in a nitrogen stream. This approach was carried out to create a defect-free surface covered by a well-defined aliphatic adsorbate layer as a reference surface to assess the impact of such aliphatic-based film on interfacial contact forces [12].

ODPA and hexyl phosphonic acid (HPA)-based organic films onto Al_2O_3(0001) single crystal were prepared by self-assembly. The freshly chemically etched and thermally annealed aluminum oxide substrates were immersed into 1 mM molecule (ODPA or HPA)-containing ethanolic solution for 12 h. The as-modified crystals were thoroughly rinsed with ultrapure ethanol, dried in nitrogen stream, and immediately used.

AFM Instrumentation

UHV-AFM

UHV AFM imaging and Force-distance curve (F-D) spectroscopy were carried out by using a VT-AFM XA (*Oxford Instruments*, Taunusstein, Germany) microscope (Fig. 2). AFM images were collected in contact mode. CSC17 cantilevers (resonant frequency of 13 kHz, spring constant of 0.18 N/m, and tip radius of 8 nm) purchased from *Mikromasch* (Bulgaria) were used. For AFM-based F-D spectroscopy measurements, data obtained from 16 × 16-point grids over 2.0 × 2.0 μm^2 areas were collected at room temperature for statistical purposes. The AFM tip was approached and retracted over the sample surface at 1 μm/s for a 500 nm tip-sample separation. The cantilevers were calibrated according to their deflection sensitivity, obtained from the slope of the repulsive regime, and the spring constant, which was obtained by means of the thermal noise method [16].

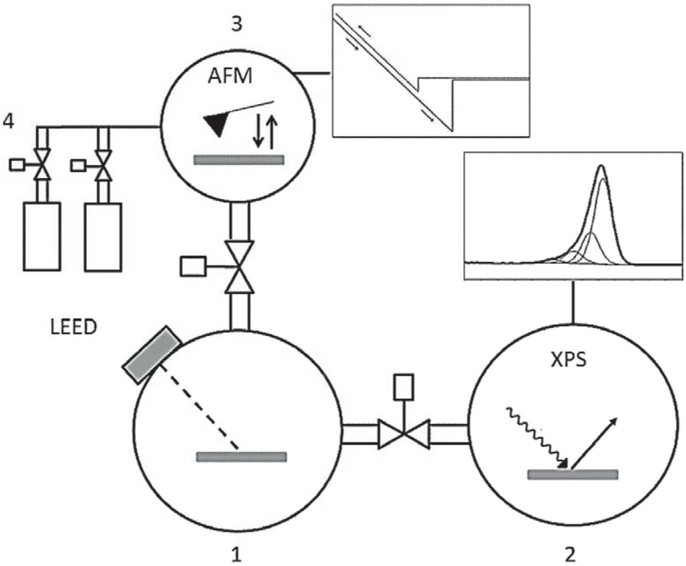

Fig. 2 Illustration of the UHV analytical setup allowing the measurement of surface chemistry and contact forces. (1) preparation chamber; (2) analysis chamber; (3) AFM chamber; (4) gas and water dosing system

Ambient Pressure AFM

AFM imaging was carried out by using a JPK Nanowizard II Ultra (*JPK Instruments AG*, Berlin, Germany) operating in air and at room temperature with a scan rate of 1 Hz. The topographical features exhibited by pristine $TiO_2(100)$ single crystal surfaces were characterized in contact mode in a window loading force range of 2–5 nN. In this case, DP17 silicon cantilevers (12 kHz, 0.17 N/m), purchased form *Mikromasch*, were used. However, for the AFM characterization of NDCA-modified $TiO_2(100)$ substrates, alternating contact mode (AC) was chosen. For the latter, an amplitude corresponding to a 90% of the free-air amplitude was maintained constant during the profiling. Both AC AFM imaging and nanoshaving experiences were carried out using NSC15 AFM tips (320 kHz, 40 N/m), acquired from *Mikromasch*. In the nanoshaving and nanografting processes, an organic molecule monolayer (typically prepared by self-assembly) is removed/altered as a consequence of AFM tip ploughing. Essentially, when high enough loading forces are applied in a pure solvent with the AFM tip, the latter is expected to scratch the modified surface and subsequently remove the organic film, unveiling thus the underlying substrate surface. This procedure is known as nanoshaving. If this process is carried out when other secondary molecules are also present in the solvent, then a fast chemisorption of the latter onto the shaved area can be obtained, i.e. nanografting [17]. It is worth noting that although the organic layer is removed as a consequence of AFM tip ploughing, no noticeable damage on the single crystalline surfaces can be detected for the loading force window range considered.

Single molecule force spectroscopy experiences on Al_2O_3(11–20) single crystals were carried out using an MFP-3D-SA (*Asylum Research*) microscope equipped with an anti-vibration system. A fluid cell (Fluid Cell Lite from *Asylum Research*) was employed to obtain the corresponding force-distance curves in 10 mM $NaClO_4$ aqueous solution at pH 6. In order to achieve good reproducibility, several hundred force curves were recorded in each experiment. The rupture events were evaluated with Igor-Pro software. Note that only a fraction (10–30%) of all curves showed rupture events. In those cases, the force recorded at the rupture point was noted and used to build an additional set of statistical data. A Gaussian fit was applied to determine the mean force value.

Modification of AFM-Tips

TiO_2 Coated AFM-Tips

NSC19 AFM cantilevers (65 kHz, 0.5 N/m), acquired from *Mikromasch*, were modified with 150 nm thick titanium coating by means of plasma-enhanced PVD. A titanium target was sputtered by a DC plasma in pure Argon atmosphere at 0.2×10^{-3} mPa at a mean power of 2 kW and 300 V bias voltage. Under these experimental conditions, a deposition rate of 14 nm/min was obtained. In order to completely oxidize the titanium coating of the cantilevers, the latter modified AFM tips were annealed in air at 600 °C for 16 h.

Macromolecular Modification of AFM Tips

Gold-coated silicon cantilevers HQ:CSC17 (13 kHz, 0.18 N/m), acquired from *Mikromasch*, were cleaned according to a well-stablished procedure published elsewhere [15]. Briefly, as-received cantilevers were immersed into an RCA-1 solution for 2 min. at 70 °C in order to remove organic contaminants. After that, the tips were rinsed with ultrapure water and subsequently dried in a nitrogen stream.

OH-Functionalization

The solvent cleaned gold-coated cantilevers were introduced into a 1 mM α-Hydroxy-ω-mercapto PEG-containing ultrapure water solution for $t = 4$ h.

NH_2 × HCl-Functionalization

The solvent cleaned gold-coated cantilevers were introduced into a 1 mM α-Mercapto-ω-amino PEG hydrochloride-containing ultrapure water solution for $t = 4$ h.

OCH_3-Functionalization

The solvent cleaned gold-coated cantilevers were introduced into a 1 mM α-Methoxy-ω-mercapto PEG-containing ultrapure water solution for $t = 4$ h.

XPS Analysis

XPS measurements were performed in an Omicron ESCA$^+$ System (Omicron NanoTechnology GmbH, Germany). The element spectra were recorded at pass energies of 25 eV. A monochromated Al Kα (1486.3 eV) X-ray source with a spot diameter of 600 μm was used. The calibration of the spectra was done by using the position of the C 1s core level peak of adventitious carbon (binding energy, BE = 285 eV) as a reference. For data evaluation, the CasaXPS software was used [18].

For the quantitative analysis of the surface chemistry of the prepared crystals, angle-resolved XPS experiments were performed. XPS spectra were recorded at take-off angles of the photoelectrons from 70° to 10° with respect to the surface plane. The probing depth d can be calculated as a function of the take-off angle Θ [19] according to $d = \lambda \sin\Theta$, where λ is the inelastic mean free path of the photoelectrons.

LEED Instrumentation

Omicron Spectra LEED optics were employed at an incident angle close to 90° with respect to the surface for LEED experiences. With the aim to obtain high-quality LEED images, the beam energy was adjusted from 80 to 120 eV. The as-registered LEED patterns of the corresponding surfaces were simulated and compared using the software LEEDpat30.

Results

Analysis of Disordered Molecular Adsorbates by Means of Nanoshaving and XPS Analysis

The molecular adsorbate formation of alkanehydroxamic and carboxylic acids on various metal oxides was investigated by Folkers et al. [20]. They observed the formation of self-assembled hydroxamic monolayers, which they attributed to the high complexation constant of the hydroxamic acids with metal ions as opposite to carboxylic acids. Thus, in the case of carboxylic acids adsorbed onto amorphous TiO_2 oxide films on Ti no self-assembly process was observed. The authors proposed that this behaviour was mainly governed by the acid to neutral behavior of the TiO_2 oxide film. Therefore, in this section we address the adsorption of model molecules with the aim of getting a good understanding of particle–wall interactions in the presence of a well-defined adsorbate under ambient conditions. Nonadecanoic acid (NDCA) was chosen as a model molecule to simulate typical adsorbates present in ambient atmosphere. The reasoning behind was that (i) the carboxylic acid group can mimic the chemical functionalities of molecules present at atmospheric conditions, (ii) the well-defined composition of the aliphatic chain results in an intense carbon signal in XPS experiments and (iii) it leads to a measurable height contrast in AFM based nanoshaving investigations. NDCA monolayers were prepared on a TiO_2(100) single crystal by self-assembly from NDCA-containing ethanolic solutions [21].

Nanoshaving

The topographical features exhibited by adsorption of NDCA molecules onto TiO_2(100) single crystal surfaces were investigated by AFM operating in air in AC mode [22]. By comparison to the smooth atomically flat terraces of pristine TiO_2(100), rounded nanostructured islands or domains decorating the terraces can be observed, which are attributable to a sub-monolayer coverage of NDCA molecules. The ploughing of a $500 \times 500\ \mathrm{nm}^2$ area with the AFM tip in contact mode with a significant high value of loading force, leads to the removal of the adsorbed NDCA molecules takes place (see Fig. 3).

As a consequence of the nanoshaving process, pristine areas of TiO_2(100) terraces are uncovered. This is an indication that the NDCA adsorbate layer is easily removed from the surface. By carrying out cross section profiles along both the outer NDCA coated and the nanoshaved areas, a corrugation of 120 pm could be measured. The latter value is noticeably lower than that expected for a tightly packed monolayer of NDCA molecules arranged in a slightly tilted standing up configuration, since the theoretical length of the NDCA molecules is in in the range of 2 nm. Consequently, the formation of a disordered film together with a low fractional surface coverage of NDCA molecules can be concluded from the analysis of the presented AFM data. These results hint at a poor interaction between the anchoring carboxylate

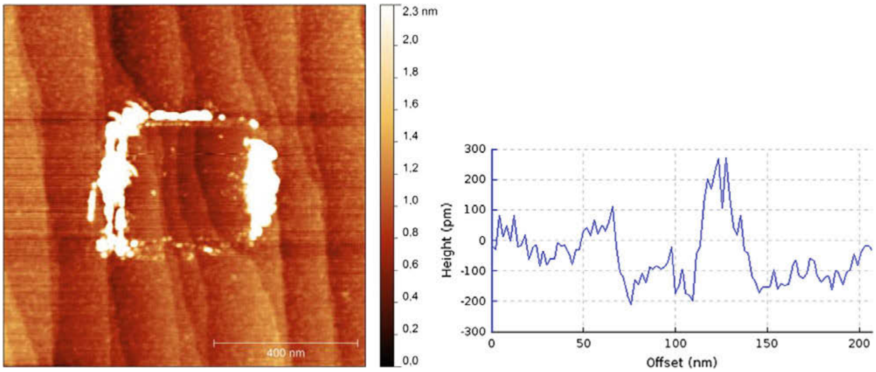

Fig. 3 *Left hand side*: Nanoshaving on an NDCA covered $TiO_2(100)$ surface shows the disordered structure of the adsorbate layer, the scan size is 1 × 1 μm^2. *Right hand side*: cross section of the area marked at the left. Reprinted from [22] with permission from Elsevier

groups and the $TiO_2(100)$ surface. The result is that NDCA molecules exhibiting carboxylate functional/anchoring groups, reversible adsorbed at active $TiO_2(100)$ adsorption sites, stay rather mobile due to relatively weak interactions.

XPS Analysis

The TiO_2 substrate was characterized by XPS before and after NDCA adsorption. The results of measurements of the pristine $TiO_2(100)$ surface measured at different take-off angles is shown in Table 1. Titanium, oxygen and carbon were found at the surface. The atomic percentage of carbon increases when the photoelectron take-off angle is decreased, which indicates that the carbon is associated to an adsorbate film formed at the crystalline surface by exposure to air (adventitious carbon).

Most importantly, in comparison to the spectrum obtained for $TiO_2(100)$ single crystals prepared in UHV conditions where the O 1s signal is exclusively originated from O^{-2} species, [23] the high resolution O 1s AR-XP core level peaks exhibit a profile with different components that can be assigned to the presence of hydroxides, adsorbed water and carboxylic groups. Indeed, the increase in the O/Ti ratio when the take-off angle is reduced hints at an oxygen enrichment of the surface supported by the surface R_{O-1}/O^{2-} and R_{O-2}/O^{2-} contributions [11], indicating a

Table 1 Surface composition of $TiO_2(100)$ surface as measured by XPS at varying take-off angles with respect to the surface plane (from [11])

Angle (°)	O 1s (at.–%) at 530.2 eV	Ti 2p 3/2 (at.–%) at 458.8 eV	C 1s (at.–%) at 285 eV
70	63.2 ± 0.5	27.9 ± 0.5	8.9 ± 0.5
40	62.5 ± 0.5	24.7 ± 0.5	12.8 ± 0.5
20	61.3 ± 0.5	19.0 ± 0.5	19.7 ± 0.5
10	51.2 ± 0.5	13.8 ± 0.5	35.0 ± 0.5

Table 2 Surface composition of the NDCA covered $TiO_2(100)$ crystal as measured by XPS at varying take-off angles with respect to the surface plane (from [11])

Angle (°)	O 1s (at.–%) at 530.2 eV	Ti 2p 3/2 (at.–%) at 458.8 eV	C 1s (at.–%) at 285 eV
70	54.1 ± 0.5	22.6 ± 0.5	23.2 ± 0.5
40	52.6 ± 0.5	18.2 ± 0.5	29.2 ± 0.5
20	41.7 ± 0.5	13.9 ± 0.5	44.4 ± 0.5
10	29.1 ± 0.5	8.9 ± 0.5	62.0 ± 0.5

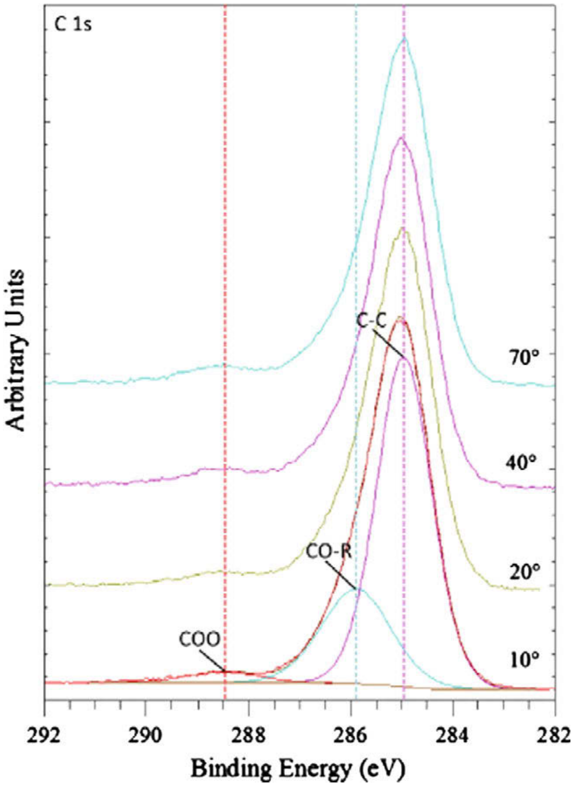

Fig. 4 C 1s spectrum of NDCA covered TiO_2 crystal at varying take-off angles. For ease of comparison, the spectra were normalized and shifted vertically. The vertical dashed lines mark the positions of the different components of the C 1s peak. Reprinted from [11] with permission from Elsevier

hydroxide-terminated surface. Consequently, it could be concluded that a layer of surface hydroxides is ubiquitously present on the $TiO_2(100)$ single crystals prepared under ambient conditions.

The adsorption of NDCA on TiO_2 could also be proven by XPS by the significantly increased carbon concentration in comparison to that exhibited by the bare $TiO_2(100)$ substrate (see Table 2).

An extensive XPS analysis of the NDCA-coated TiO_2 crystals exhibited a C 1s signal with a peak width of 1.25 eV of the C–C component at a takeoff angle of 10° as depicted in Fig. 4.

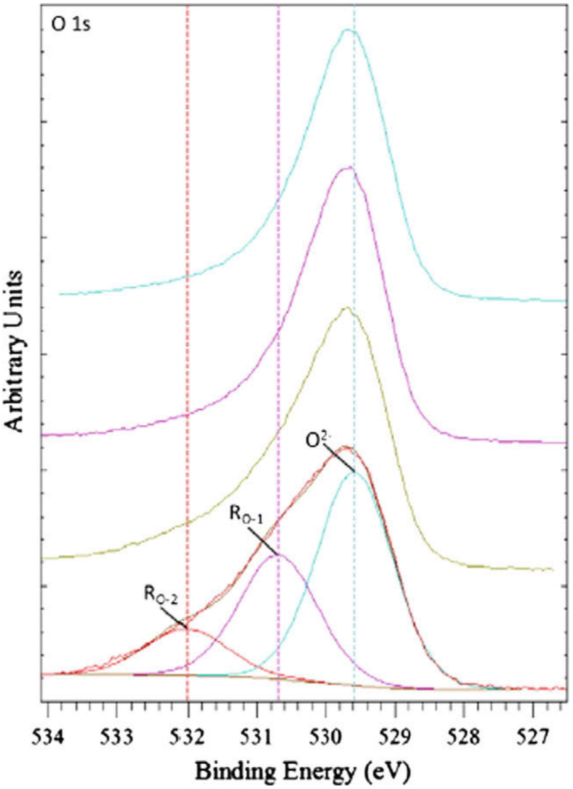

Fig. 5 O 1s spectra of the NDCA covered $TiO_2(100)$ surface measured at the same take-off angles as in Fig. 4. For ease of comparison, the spectra were normalized and shifted vertically. Reprinted from [11] with permission from Elsevier

The as-prepared NDCA adsorbate film exhibits the characteristic C 1s spectrum expected for a long chain carboxylic acid, as can be seen in Fig. 4. The registered ratio of C–C/COO is close to 16–18 range, which corresponds to the expected stoichiometry of NDCA. Thus, the undefined original layer of adventitious carbon has been replaced in this case by a well-defined layer of NDCA molecules, most likely due to the stabilizing effect of intermolecular long aliphatic chain van der Waals interactions.

Additionally, the detailed assessment of the components present in the O 1s signal, displayed in Fig. 5, together with the corresponding atomic fraction shown in Table 3, allows to conclude that the underlying $TiO_2(100)$ single crystalline surface still exhibits the same $OH{:}O^{2-}$ ratio as the pristine crystalline surface (Table 1). A slightly reduced value of the O/Ti ratio is seen in this case, which is attributed to the displacement of adsorbed water molecules by NDCA.

XPS characterization reinforces the observation that NDCA molecules chemisorb porly onto the $TiO_2(100)$ single crystalline surfaces due to weak interactions occurring between the hydroxyl-stabilized TiO_2 surface and anchoring carboxylate groups. Indeed, taking into account the presented data, no condensation between the latter and hydroxyl groups present in the substrate surfaces can be detected. Consequently,

Table 3 Detailed composition of the O 1s element spectra of the NDCA covered surface at varying take-off angles (from [11])

Angle (°)	$\underline{O}_{\Sigma}$/Ti	$\underline{O^{2-}}$/Ti	$\underline{O}H/O^{2-}$	$(H_2\underline{O}, C\underline{OO}H)/O^{2-}$
70	2.4	2.0	0.16	0.05
40	2.8	2.1	0.24	0.08
20	3.0	2.0	0.32	0.16
10	3.3	1.8	0.60	0.24

the ubiquitous presence of these hydroxyl groups, together with water adsorbate layers, on the TiO_2 surface (prepared in ambient conditions) is tentatively proposed to be responsible for the formation of the poorly packed and disordered NDCA layer initially observed by AFM and XPS and lately supported by AFM nanoshaving. This argument is additionally supported by Henderson et al. who reported the dissociation of water molecules on TiO_2(100) surfaces to give rise to two hydroxide groups adsorbed onto the surface: the first one to Ti^{4+} adsorption sites, whilst the second one would be bound at bridging O^{2-} [24]. It has also been proposed that the adsorption of volatile molecules could also take place by forming Ti–O bonds [25]. The latter, together with the above-mentioned hydroxide groups and the water adlayers, would strongly inhibit the anchoring of carboxylate groups to this TiO_2(100) surface prepared in ambient conditions.

Conclusions

A new methodology for the preparation of rutile TiO_2(100) crystalline surfaces in water and oxygen partial pressures at high temperature is reported. Apart from small amounts of carbon-based contamination bearing carboxylate moieties (i.e. organocarboxilate adsorbates coming from the laboratory atmosphere), angle-resolved XPS shows the presence of a hydroxyl layer terminating the single crystal surface. Hydroxyl groups are proposed to chemisorb preferentially at defects present on the TiO_2(100) surface lowering thus the surface energy.

The adsorption of NDCA molecules onto the as-prepared bare TiO_2(100) surfaces results in the displacement of the adventitious carbon layer typically present at surfaces exposed to air and resulted in a noticeable rise in the contact angle from 18 ± 3° to 45 ± 3° [12]. The combination of angle-resolved-XPS and AFM nanoshaving allows to conclude that a disordered adsorbate layer of NDCA molecules essentially lying flat on the substrate terraces is formed (as opposed to the formation of a self-assembled monolayer). Consequently, nanoshaving has been shown to be a reliable method for the fundamental characterization of adsorbate layers. In the particular case of NDCA-coated TiO_2(100) substrates, nanoshaving unveiled disordered organic layer exhibiting a fractional surface coverage consistent with a submonolayer.

The presence of terminating hydroxyl groups, together with water adlayers, on the as-prepared TiO_2(100) crystalline surface strongly inhibits the formation of well-defined tightly packed and ordered NDCA monolayers. Consequently, weak interactions between the anchoring carboxylate groups and the hydroxyl-stabilized $TiO_2(100)$ terraces, namely hydrogen bridging, are proposed to be responsible for the observed behaviour.

Nanoshaving and Nanografting of ODPA Monolayers on Al_2O_3 Surfaces [22]

The combination of nanografting and nanoshaving techniques can be considered a valuable tool to assess the quality of self-assembled monolayers. The characterization of a vast variety of spontaneously adsorbed molecules on noble metals has been carried out by means of AFM-based nanografting over the last few years [26–28]. In particular, the impact exerted by different distal functional groups and chain lengths on frictional coefficients has been assessed by nanografting. In addition, the differential adsorption of thiol molecules by means of either nanografting or self-assembly has been compared [27, 28]. Most importantly, it has been stated that as a consequence of the reduced spatial confinement, fewer pinholes and defects can be obtained in the grafted patches in comparison to those obtained in the outer self-assembled molecule layer regions [28]. In this regard, nanografting appears as a very reliable and useful technique for the characterization and modelling of the molecular adsorption and self-assembly processes at the nanoscale. Indeed, when the spontaneous chemisorption of certain molecules exhibiting enhanced affinities for specific surfaces is considered (for instance aliphatic thiols on gold), then the suitability of using in situ-AFM measurements for the monitoring of the monolayer assembly decreases. In the following, nanografting and nanoshaving processes have been carried out to characterize the adsorption of phosphonate-terminated aliphatic molecules onto $Al_2O_3(0001)$ single crystals. The study was supplemented with XPS measurements of the surfaces.

High-resolution AFM images registered in both contact and AC mode for the bare Al_2O_3 single crystals measured in ambient conditions are displayed in Fig. 6. The solvent-cleaned substrates exhibited a relatively smooth surface which turned into characteristic atomically flat terraces after etching and thermal annealing. Similar results to these presented in this chapter have been reported elsewhere [29, 30]. These terraces are in the range of ~1 μm wide. However, the methodology employed for the preparation of this multistep terraced morphology brought about some inhomogeneities, even when analogue $Al_2O_3(0001)$ substrates were submitted to identical experimental conditions. These particular results can be summarized as follows: (i) typical morphological features, involving multistep ~1 μm-wide atomically flat terraces, were obtained for all the samples measured, as can be seen in the topographical AFM images depicted in Fig. 6a, c, e; however, (ii) noticeable heterogeneities were then unveiled by both friction (Fig. 6b, f), and phase contrast images (Fig. 6d).

These results can be tentatively interpreted as follows. When working in ambient conditions, water adlayers adsorbed onto the surface are expected to modify signifi-

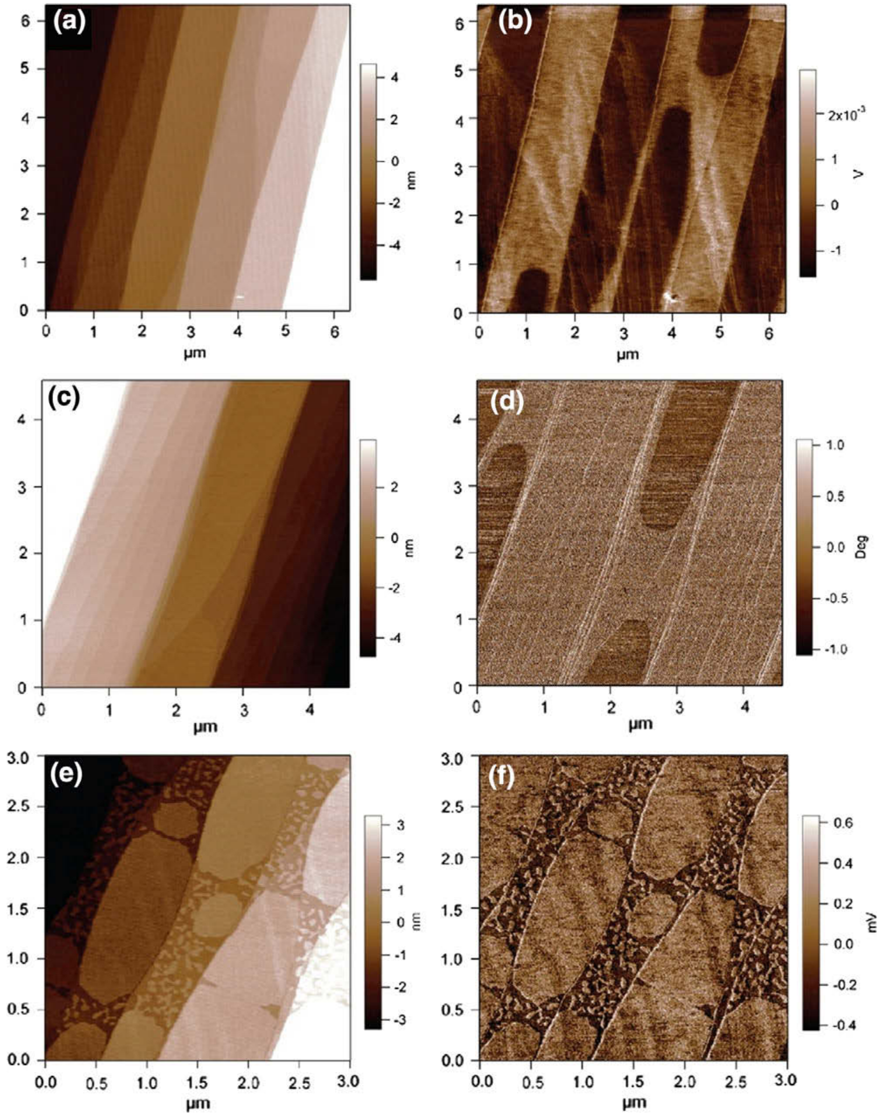

Fig. 6 AFM images showing morphological differences and heterogeneities on $Al_2O_3(0001)$ surfaces. **a** and **c** Topography images of typical atomically flat terraces. **b** Friction and **d** phase images reveal different terminations on the same terrace. **e** and **f** Similarly prepared single crystals showing domains (**e** topography image; **f** friction image). The measurements were performed under ambient conditions. Reprinted from [22] with permission from Elsevier

cantly the tip-to-surface interaction contact forces. In this context, although the height differences, which can be obtained from topographical AFM images by performing cross section profiles, are in the range of ~100 pm, noticeable phase and friction contrast showing well-defined domains can be observed in Fig. 6b, d, f. The latter could then be attributed to the presence of water adsorbate layers on the crystalline surfaces. Interestingly, large rounded and elongated domains seem to coexist with smaller and amorphous islands (see Fig. 6e). Consequently, the presence of these domains definitely accounts for a differential friction behaviour which is eventually indicative of a different surface termination. However, AFM experiments carried out in UHV at 140 °C showed the persistence of these friction-contrast domains even at high temperature, i.e. presumably in the absence of physisorbed water [22]. The origin of the heterogeneities revealed by phase and friction contrast AFM imaging is unclear. In the following, fot the sake of simplification, the morphologies shown in Fig. 6b and d will be identified as *type 1*, whilst those displayed in Fig. 6f will be named *type 2*. It is worth noting that previous studies carried out onto $Al_2O_3(0001)$ single crystals in UHV conditions pointed out to two distinct surface terminations, i.e. Al and O [31]. Additionally, AFM-based studies, also performed in UHV, have demonstrated a hexagonal conformation for two layers of Al atoms for these crystalline facets [32]. However, in contrast to the surfaces obtained in UHV conditions, single crystalline $Al_2O_3(0001)$ substrates prepared in ambient experimental conditions exhibit a differential surface composition since they are exposed to both oxygen activity and water adlayers. Indeed, it has been widely stated that hydroxide-coated alumina crystalline surfaces are the most stable configurations under ambient conditions since hydroxylation is expected to decrease the surface energy of aluminium oxide [33]. Thus, in the absence of water, Al and O surface terminations would be expected. However, aluminium oxide surfaces are expected to suffer hydroxylation in water-containing ambient condition as published elsewhere [29]. In fact, the existence of hydroxyl-stabilized $Al_2O_3(0001)$ terraces in the alumina substrates etched and annealed in ambient (water containing) conditions has been proved by XPS, shown in Fig. 7.

Once the adsorption of octadecylphosphonic acid (ODPA) molecules (from ethanol) on the as-treated $Al_2O_3(0001)$ terraces (after etching and annealing in ambient conditions) has taken place, AFM nanoshaving was performed onto the ODPA-modified alumina single crystal. In this context, AFM imaging carried out onto the latter modified substrate and displayed in Fig. 8a shows the formation of a very homogeneous and closely packed ODPA layer. A representative cross section profile taken in the AFM image depicted in Fig. 8a point at two terraces, indicated with stars, exhibiting a rougher surface, in contrast with the other much smoother surrounding terraces. This fact has been tentatively attributed to weak interactions between the phosphonate anchoring groups and the $Al_2O_3(0001)$ terraces giving rise to a disordered and poorly bound ODPA layer. Conversely, a stronger interaction with the $Al_2O_3(0001)$ surface together with the formation of a compact and tightly packed ODPA film on the smoother terraces is proposed.

Taking this fact into account, for the following an ODPA-modified $Al_2O_3(0001)$ substrate exhibiting the afore-mentioned two types of organic films (disordered and

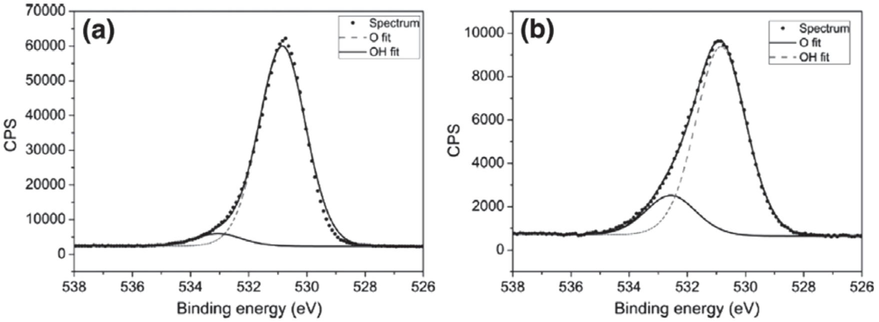

Fig. 7 XPS measurements of the O 1s region of the $Al_2O_3(0001)$ single crystal at **a** 70° and **b** 20° take-off angle. The spectra were fitted with two components assigned to oxide (at lower binding energy) and hydroxide species (at higher binding energy positions). A clear increase of the hydroxide contribution was found for the spectrum acquired with a lower take-off angle, indicating that the hydroxide lies on top of the surface. Reprinted from [22] with permission from Elsevier

compactly packed) is considered, as can be seen in the white rectangle area indicated in Fig. 8b. By applying with the AFM tip a high enough loading force in contact mode to the ODPA-modified aluminum oxide single crystal, the organic layer is completely removed unveiling thus the underlying substrate surface, i.e. nanoshaving, see the ploughed squared area in Fig. 8c. The as-detached ODPA molecules rapidly diffuses to the bulk ethanolic solution and no readsorption is detected at all. Cross section profiles carried out through the "shaved" and surrounding areas in the same terrace allows to accurately quantify the thickness of the ODPA layer. Thus, the as-measured thicknesses in both differentiated regions (1 and 2 as identified in Fig. 8b) reaches a value of ~2.0 nm which is quite close to the theoretical length calculated for the ODPA molecule. The latter is therefore indicative of ODPA monolayer film formation in a slightly tilted standing-up configuration in the two different areas shown in Fig. 8b. Most importantly, after successive AFM scanning on the same area, only ODPA molecules strongly adsorbed on the ordered and well-packed domains on the $Al_2O_3(0001)$ terraces remain adsorbed, while those weakly adsorbed in disordered ODPA regions are subsequently removed as can be observed in Fig. 8d. This result hints at the fact that ODPA molecules can presumably bind strongly to just one single type of surface termination. Conversely, physisorption is most likely to occur on the other crystalline surface termination.

Nanografting experiments have been carried out on hexylphosphonic acid (HPA)-modified $Al_2O_3(0001)$ single crystals by using longer aliphatic chain ODPA molecules. More stable self-assembled monolayers can be obtained for phosphonate-terminated molecules incorporating longer aliphatic chain due to the enhanced intermolecular van der Waals interactions. After nanoshaving the squared area displayed in Fig. 9a of an HPA-modified $Al_2O_3(0001)$ in a 1 mM ODPA-containing ethanolic solution, the grafting of ODPA molecules in the "shaved" area, where HPA molecules have been desorbed by AFM ploughing, has taken place. The latter can be justified in terms of the brighter squared area corresponding to higher regions observed in

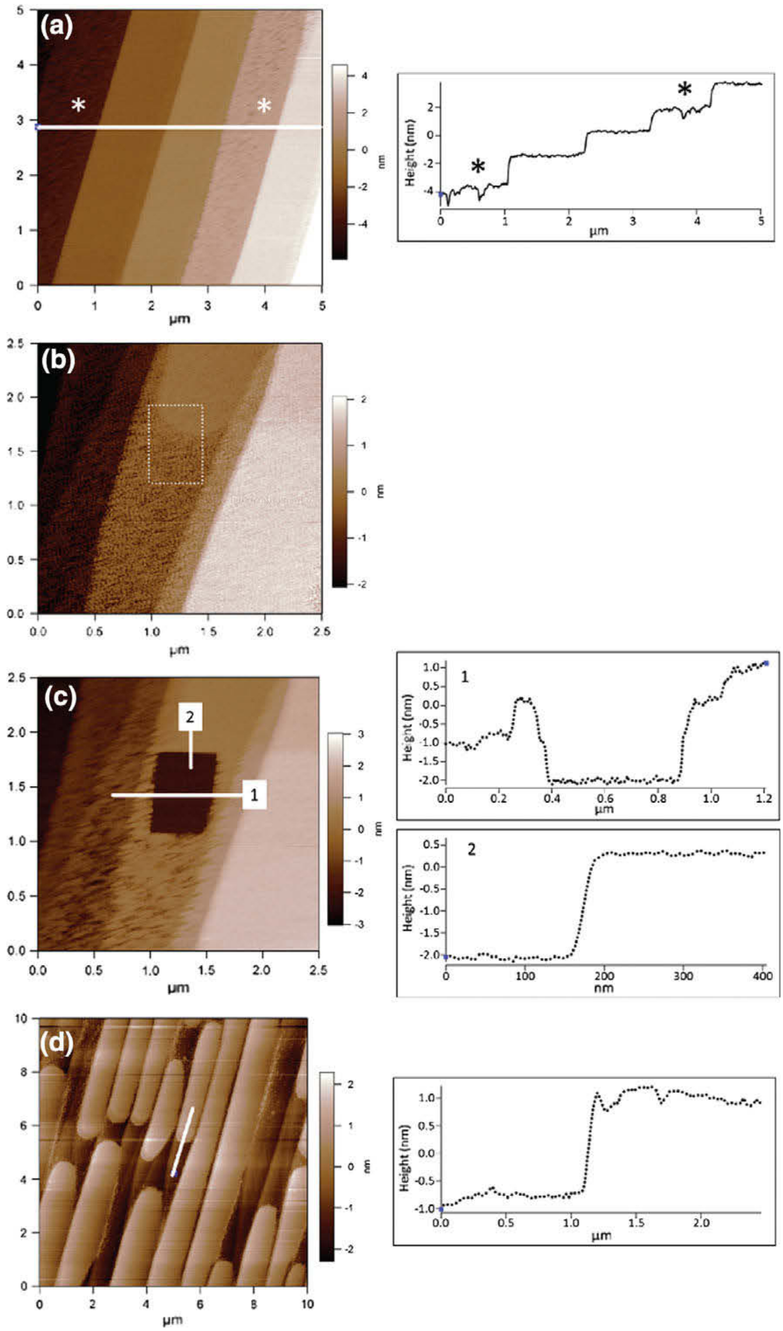

Fig. 8 **a** AFM topography of ex-situ adsorbed ODPA on $Al_2O_3(0001)$. Topography **b** before and **c** after nanoshaving on an area containing two different surface terminations. **d** Same crystal after two AFM scans. ODPA stays stable only on one type of surface termination. The measurements were performed in ethanol. Reprinted from [22] with permission from Elsevier

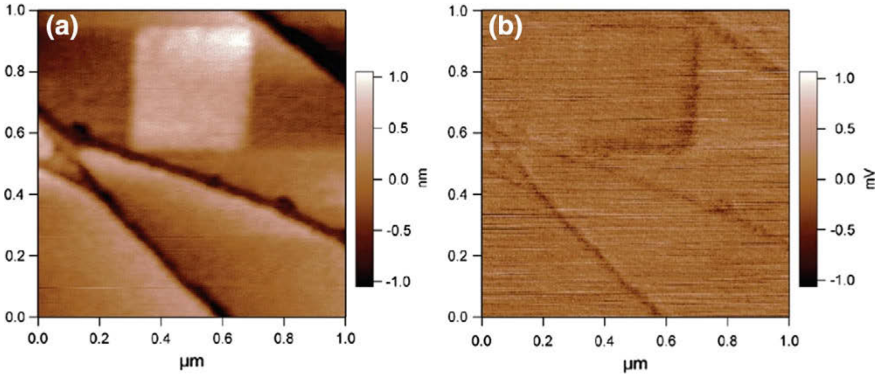

Fig. 9 Nanografting on Al_2O_3 single-crystal surfaces. **a** Topography and **b** friction images after nanografting in the presence of ethanolic ODPA solution on the HPA-covered (0001) surface. Reprinted from [22] with permission from Elsevier

Fig. 9a. Since both molecules, i.e. HPA and ODPA, are CH_3-terminated, no remarkable differences could be found in the AFM friction image (see Fig. 9b). Cross section profiles performed through the squared and surrounding areas exhibit a positive height difference of 0.8 nm which is slightly lower but reasonably consistent with the difference between the theoretical lengths of HPA and ODPA [22].

The results of the afore-mentioned experiments accounts for the systematic characterization of the adsorption processes and self-assembly kinetics of phosphonate-terminated aliphatic molecules on model aluminum oxide crystalline surfaces. The preparation (chemical etching and thermal annealing) of Al_2O_3(0001) single crystalline surfaces upon exposure to ambient conditions brought about surface heterogeneities corresponding to a differential surface termination. The latter determines the nature of the bonding interaction between the adsorbed molecule and the aluminum oxide surface and, consequently, both the ordering and density of the packing arrangement into a film, as reliably demonstrated by nanoshaving. Additionally, nanografting has been shown to be a useful and reliable technique for studying both adsorption and self-assembly kinetics of phosphonate-based moieties at the liquid/metal oxide interface.

Investigation of TiO_2–TiO_2-Contact Forces Under UHV Conditions

Contact forces between micro- and nanoparticles can be accurately estimated by force spectroscopy measurements using an atomic force microscope (AFM). As previously stated, under ambient conditions particle-to-particle interactions are significantly influenced by the formation of capillary forces. Indeed, Farshchi-Tabrizi et al. [7]

showed that the contact geometry exerts a significant influence on the dependence between relative humidity and adhesion forces. Additionally, the superficial chemical composition of TiO_2 can be modified by water adlayers and by exposure to UV-light, which may result in remarkable modifications of adhesion behavior [34]. However, under ultrahigh vacuum conditions (UHV) experimental conditions, capillary bridges do not form and particle-particle contact force interactions can be then evaluated for well-defined surface chemistries. To the best of our knowledge only a few works based on the study of contact forces via an UHV AFM have been reported so far [35].

TiO_2 single crystalline surfaces provide an excellent platform as a model system for studying adhesion phenomena due to their well-defined atomic surface structure. Within this section, the contact forces between a TiO_2-coated AFM tip and a rutile $TiO_2(110)$ single crystalline surface in different chemical states were investigated under UHV-conditions in order to address particle-wall interactions under well-defined experimental conditions [12]. Additionally, particle-wall contact forces were measured between TiO_2-coated AFM tips and $TiO_2(110)$ single crystal modified with an octadecylphosphonic acid (ODPA) monolayer. The coating with ODPA provided a defect-free reference system, and also prevented from ulterior additional uncontrolled adsorption by exposure to air, due to the low surface energy of the ODPA-coated $TiO_2(110)$.

Both the surface chemistry of the TiO_2 films grown on the AFM cantilevers and $TiO_2(110)$ single crystalline surfaces were modified in situ by argon ion bombardment at low energy, water dosing at 3×10^{-6} Pa, and an annealing step at 200 °C. These treatments led to measurable differences in the density of Ti(III) defect states by XPS (note that the transfer between the AFM setup and the XPS measurement position were done without breaking UHV conditions). The measured contact forces could be correlated to the surface defect density. The results are discussed as function of electronic structure changes and their influence on the Hamaker constant.

XPS and UPS Investigation of the Surface

High-resolution Ti 2p spectra registered for a $TiO_2(110)$ single crystal before and after the Ar^+ bombardment are displayed in Fig. 10a, b, respectively. It should be noted at this point that the XPS characterization of TiO_2-coated AFM cantilevers and $TiO_2(110)$ single crystals showed no large differences between the two oxide surfaces. Most importantly, after Ar^+ bombardment treatment, both types of TiO_2 showed an increase of surface defect density, identifiable by the appearance of Ti(III) states (around 20% of the original titanium changed to the Ti(III) oxidation state after bombardment). This effect has been attributed to the transfer of one electron to Ti 3d empty levels during the formation of surface defects created by Ar^+ bombardment [36].

The Ti 2p core level spectra displayed in Fig. 10b corresponds to the successive surface treatment experienced by the TiO_2 single crystal, namely Ar^+ bombardment, water dosing at 3×10^{-6} Pa, and annealing at 200 °C. The as-registered spectra